Journal of Reproduction and Development, Vol. 62, No 4, 2016

—Original Article—

Gene expression patterns in granulosa cells and oocytes at various stages of follicle development as well as in *in vitro* grown oocyte-and-granulosa cell complexes

Yasuhisa MUNAKATA[1)], Ryoka KAWAHARA-MIKI[2)], Shogo SHIRATSUKI[1)], Hidetaka TASAKI[1)], Nobuhiko ITAMI[1)], Koumei SHIRASUNA[1)], Takehito KUWAYAMA[1)] and Hisataka IWATA[1)]

[1)]*Department of Animal Sciences, Tokyo University of Agriculture, Kanagawa 243-0034, Japan*
[2)]*NODAI Research Institute Genome Research Center, Tokyo University of Agriculture, Tokyo 156-8502, Japan*

Abstract. Follicle development is accompanied by proliferation of granulosa cells and increasing oocyte size. To obtain high-quality oocytes *in vitro*, it is important to understand the processes that occur in oocytes and granulosa cells during follicle development and the differences between *in vivo* and *in vitro* follicle development. In the present study, oocytes and granulosa cells were collected from early antral follicles (EAFs, 0.5–0.7 mm in diameter), small antral follicles (SAFs, 1–3 mm in diameter), large antral follicles (LAFs, 3–7 mm in diameter), and *in vitro* grown oocyte-and-granulosa cell complexes (OGCs), which were cultured for 14 days after collection from EAFs. Gene expression was analyzed comprehensively using the next-generation sequencing technology. We found top upstream regulators during the *in vivo* follicle development and compared them with those in *in vitro* developed OGCs. The comparison revealed that *HIF1* is among the top regulators during both *in vivo* and *in vitro* development of OGCs. In addition, we found that HIF1-mediated upregulation of glycolysis in granulosa cells is important for the growth of OGCs, but the cellular metabolism differs between *in vitro* and *in vivo* grown OGCs. Furthermore, on the basis of comparison of upstream regulators between *in vivo* and *in vitro* development of OGCs, we believe that low expression levels of *FLT1* (VEGFA receptor), *SPP1*, and *PCSK6* can be considered causal factors of the suboptimal development under *in vitro* culture conditions.
Key words: Early antral follicle, Granulosa cells, Oocytes

(**J. Reprod. Dev. 62:** 359–366, 2016)

During development of an oocyte, its size rapidly increases from the early antral follicle (EAF) stage to the antral follicle (AF) stage; this process takes 2 weeks in pigs and cows. Follicle development is accompanied by a remarkable increase in the number of granulosa cells, such that EAFs contain only thousands of granulosa cells, whereas AFs contain at least one hundred thousand granulosa cells [1]. Granulosa cells support oocyte development in a paracrine and autocrine manner [2].

Because of structural limits, including the presence of theca layers, angiogenesis does not occur in the inner follicle milieu [3], and thus, the supply of energy and oxygen depends only on diffusion, which may make the inner follicular conditions hypoxic. The granulosa cell number is a key determinant of the follicular oxygen concentration [4], and in a mathematical model, the oxygen concentration in follicles was predicted to be low [5, 6]. In addition, the oxygen concentration in human follicular fluids was found to be 1.3–5.5% [7]. These results suggest that rapid proliferation of granulosa cells in follicles occurs during hypoxia.

Received: February 8, 2016
Accepted: March 30, 2016
Published online in J-STAGE: April 22, 2016

Correspondence: H Iwata (e-mail: h1iwata@nodai.ac.jp)

Cellular proliferation requires energy, and the cellular energy depends on glycolysis for anaerobic production of ATP and pyruvate in the cytoplasm as well as on oxidative phosphorylation (OXPHOS) for aerobic production of ATP in mitochondria. Cells can vary the proportion of the methods of energy production such that some cancer cells switch the metabolic pathway to glycolysis due to a lack of angiogenesis [8]; this switch is a major factor that supports their proliferation [9]. In this context, however, it is unclear how the proliferation of granulosa cells during follicular development is supported.

Lately, immature follicles are considered useful genetic resources, and development of culture methods to induce immature oocytes to grow to the full size has been the goal of many researchers. Nonetheless, quality of oocytes grown *in vitro* and the efficiency of the culture system are still low. To shed light on the causal factors of the impaired oocyte development *in vitro*, there is a need for a comparison of gene expression patterns in granulosa cells and oocytes with the expression in their developing *in vivo* counterparts. In the present study, we showed the intrinsic changes in gene expression patterns of granulosa cells and oocytes during the development from EAFs to large AFs (LAFs) in swine. We also compared the gene expression patterns of oocytes grown *in vitro* and in the surrounding granulosa cells with such patterns in their counterparts that developed *in vivo*. The comparison revealed active glycolysis-mediated gene expression in granulosa cells during follicle development and identified the key factors that can improve development under *in vitro* culture conditions.

Materials and Methods

Reagents and media

All the reagents were purchased from Nacalai Tesque (Kyoto, Japan), unless otherwise stated. The medium used for the *in vitro* growth of oocyte-and-granulosa cell complexes (OGCs) was the α-minimum essential medium (αMEM; Sigma-Aldrich, St. Louis, MO, USA) supplemented with 10 mM taurine, 1 μg/ml 17β-estradiol, 0.1 mAU/ml FSH (Kawasaki Mitaka, Tokyo, Japan), 2% polyvinylpyrrolidone-360K (Sigma-Aldrich), 2 mM hypoxanthine (Sigma-Aldrich), 1% insulin-transferrin-selenium (Gibco BRL, Grand Island, NY, USA), 3 mg/ml bovine serum albumin (Fraction V), and antibiotics (100 μg/ml streptomycin and 10 IU/ml penicillin).

Collection of ovaries

The porcine ovaries were collected from prepubertal gilts at a local abattoir and transported to the laboratory (at approximately 37ºC in phosphate-buffered saline [PBS] containing antibiotics) within 1 h.

Collection of OGCs from EAFs

The ovarian cortical tissues were excised from the ovarian surface, and OGCs were collected from EAFs (0.5–0.7 mm in diameter) under a dissection microscope. The OGCs were further cultured for 14 days or subjected to gene expression analysis. To prepare oocytes and granulosa cells for gene expression analysis, oocytes were removed from the OGCs with a narrow pulled pipet, and each oocyte and granulosa cell was subjected to massively parallel high-throughput RNA sequencing (RNA-Seq). A total of 200 oocytes and surrounding granulosa cells were prepared for the analysis.

Collection of cumulus cell-and-oocyte complexes (COCs) from small AFs (SAFs) and LAFs

Follicle contents were aspirated from SAFs (1–3 mm in diameter) and LAFs (3–5 mm in diameter) using a syringe connected to a 21-gauge needle. The same ovaries were used as those that we used for EAF collection. After aspiration, COCs were collected from the follicular contents, transferred to PBS containing 0.1% hyaluronidase, and vortexed for 5 min to obtain denuded oocytes and granulosa cells. A total of 200 oocytes and corresponding granulosa cells collected from each SAF and LAF were used for the gene expression analysis.

In vitro growth of the OGCs

OGCs from EAFs (Fig. 1-A) were individually cultured in 200 μl of the culture medium in 96-well plates (Falcon 353072; BD Biosciences, Franklin Lakes, NJ, USA) for 14 days. A half of the medium was replaced with a fresh one at 4-day intervals. *In vitro* culture of OGCs was maintained at 38.5ºC in the atmosphere of 5% CO_2 and 95% air. At the end of the culture period (14 days), OGCs with antrum cavities (Fig. 1-C) were further analyzed. The oocytes grown *in vitro* were removed from OGCs using narrow pulled pipettes, and the each oocyte and granulosa cell mass was subjected to the gene expression analysis. Two hundred oocytes and surrounding granulosa cells that developed *in vitro* were used for the gene expression analysis.

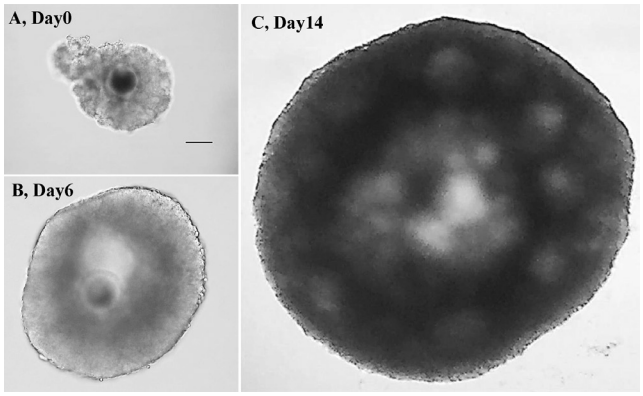

Fig. 1. Representative pictures and images of oocyte-and-granulosa cell complexes (OGCs) cultured *in vitro*. OGCs were collected from early antral follicles (EAFs) (A) and cultured for 14 days. During the culture period, OGCs formed antrum like cavities and grew in size (panel B: Day 6 and panel C: Day 14). After 14 days, OGCs forming pseudo antrum cavities were selected (C). The scale bar is 100 μm.

Transcriptomic analysis

Total RNA was extracted using the RNAqueous kit (Life Technologies, Carlsbad, CA, USA) from oocytes or granulosa cells of EAFs, SAFs, LAFs, and *in vitro* grown OGCs (IVGs). A total of 20 gilts were used for collection of OGCs, and 200 oocytes were analyzed from each developmental stage. After an RNA quality check using a 2100 Bioanalyzer (Agilent Technologies, Palo Alto, CA, USA), cDNA libraries were prepared using the TruSeq RNA Sample Preparation Kit (Illumina, San Diego, CA, USA). Quality and quantity of the libraries were examined using an Agilent 2100 Bioanalyzer and the KAPA Library Quantification Kit (KAPA Biosystems, Wilmington, MA, USA), respectively. From these libraries, clusters were generated on a cBot (Illumina), and two lanes for the eight groups were sequenced as 50-bp reads (single end) on a HiSeq 2500 (Illumina). Image analysis, base calling, and quality filtering were performed in the CASAVA software version 1.8.3 (Illumina) following the manufacturer's instructions. The resulting sequence data were filtered to discard the adapter sequence, ambiguous nucleotides, and low-quality sequences. After that, the retained sequence data were aligned to the swine genome sequence (susScr3) to count the sequence reads. On the basis of the mapped sequence data, calculation of the expression value for each gene and statistical analysis of differentially expressed genes were performed. Filtering, mapping, and subsequent analysis were performed by means of the CLC genomics workbench (Qiagen, Redwood City, CA, USA). For prediction of upstream transcriptional regulators, genes that were significantly differentially expressed were analyzed using the Upstream Regulator function of Ingenuity Pathway Analysis (IPA, Qiagen). IPA determined how many known targets of each transcription regulator were present in the differentially-expressed-gene list, and calculated the overlapping P-value to measure the statistically significant overlap. Fisher's exact test was used for the analysis enrichment of a gene set in the functional categories, and significance was generally assumed at P-values less than 0.01. IPA also compared the direction

of the gene expression change to infer the activation status of the predicted transcriptional regulators. On the basis of the observed differential regulation of a gene in the differentially-expressed-gene set, the activation status of an upstream regulator was determined by the direction associated with the relation from the regulator to the gene. We then determined "Z-scores", which determine whether an upstream transcription regulator has significantly more "activated" predictions than "inhibited" predictions ($z > 0$) or vice versa ($z < 0$). The data on the gene expression analysis were deposited in the DDBJ Sequence Read Archive (accession ID: DRA004449).

Quantitative reverse transcription real-time PCR

To validate the results of the next-generation sequencing (NGS) analysis, we conducted RT-PCR for *FLT1, SPP1, HIF1, VEGF,* and *ACTN4* and compared relative expression levels among follicle developmental stages. On the basis of the NGS data, we found that the expression levels of almost all housekeeping genes (e.g., *B-ACTIN, H2A* family members, *HPRT1, PGK1, GAPDH,* and *ATP5F1*) changed significantly during follicular development. Thus, we selected *GPX7* as the reference gene because of its high and constant expression level during follicular development from EAFs to LAFs. Fold changes between the different follicle stages were 1.001-fold for EAFs/SAFs ($P = 0.88$) and 0.845-fold for SAFs/LAFs ($P = 0.35$). Given that the expression level of *GPX7* significantly differed between IVGs and SAFs and between LAFs and IVGs, and because we could not find other genes that showed high and constant expression levels at all stages (EAFs, SAFs, LAFs, and IVGs), we compared the relative expression levels of the genes in the EAFs, SAFs, and LAFs. Granulosa cells were collected from OGCs of 20 EAFs, SAFs, and LAFs as described above, and three samples were prepared from different ovary series. RNA was extracted from oocytes using an RNA isolation kit (RNAqueous-Micro, Ambion, Applied Biosystems, Austin, TX, USA). The extracted RNA was reverse-transcribed into cDNA using the Thermo script RT-PCR system (Invitrogen). The primer for the reverse transcription was the oligo$(dT)_{20}$ included in the kit. Quantification of cDNA was then performed by real-time PCR using the Rotor-Gene 6500 system. The forward and reverse primers for *FLT1*, *SPP1*, *HIF1*, *VEGF*, *ACTN4*, and *GPX7* were designed using DDBJ (http://arsa.ddbj.nig.ac.jp/top-j.html) and Primer3 (http://frodo.wi.mit.edu/primer3/). The primer sets were FLT1: 123-bp amplicon, CGTGGCTTCCAACAAAGTGG and GACAGCTTCAGGTCTTCCCC; SPP1: 138-bp amplicon, AGTCCAACGAAAGCCCTGAG and CGGAGTGATGAGACTCGTCG; HIF1: 144-bp amplicon, AGCCAGATGATCGTGCAACT and CCATTGATTGCCCCAGGAGT; VEGFA: 129-bp amplicon, TCGGAGCGGAGAAAGCATTT and CGGCTTGTCACATCTGCAAG; ACTN4: 132-bp amplicon, CGACCACTTGGCAGAGAAGT and TTGCGGATGAGGGCTTTGAT; and GPX7: 95-bp amplicon, GGGCGGAAAAGTCTAGCAGT and GGCTGGTGAATGACTGGTCA. Each PCR involved an initial denaturation step of 95°C for 1 min followed by 40 cycles of 98°C for 5 sec and 59°C for 11 sec. SYBR green fluorescence was measured at the end of each extension step (59°C). A melting curve was analyzed to check specificity of the PCR products, and agarose gel electrophoresis was carried out to verify the amplicon sizes. Relative gene expression levels of each gene of interest were calculated via normalization to the expression levels of the endogenous control: *GPX7*. The reactions were run in duplicate, and the experiments were repeated three times for each cellular series. For each PCR run, a standard curve was generated using serial 10-fold dilutions of the corresponding standard plasmid of a known concentration.

Statistical analysis

The ratios of the number of genes with significant up and downregulation associated with HIF1, glycolysis, and OXPHOS were compared using chi-squared tests. Comparison of the relative-gene-expression data obtained by RT-PCR between EAFs and SAFs and between SAFs and LAFs involved Student's *t*-test. Differences with P-values less than 0.05 were considered statistically significant.

Results

Comparison of NGS data with those of real-time RT-PCR analysis

Relative expression levels of *FLT1, SPP1, HIF1, VEGF,* and *ACTN4* as compared to the expression of *GPX7* are shown in Table 1. We found that the expression patterns of the genes were almost identical between the RT-PCR data and NGS data.

Top five upstream regulators in granulosa cells and oocytes during follicle development in vivo and in vitro

The gene expression of granulosa cells was compared between SAFs (*in vivo* grown OGCs from SAFs) and IVGs (*in vitro* grown OGCs) and between LAFs (*in vivo* grown OGCs from LAFs) and IVGs; 483 and 410 statistically significant upstream regulators were predicted using Ingenuity Upstream Regulator Analysis as implemented in IPA. The top five of these upstream regulators in granulosa cells are shown in Table 2. The comparison revealed that the common upstream regulators were TP53, HIF1A, and SP1. All of these factors are important for follicular development; thus, TP53, HIF1A, and SP1 are also predicted to be upstream regulators in both follicular developmental periods: from EAFs to SAFs and from SAFs to LAFs (Table 3). Table 4 shows the top five upstream regulators of *in vitro* and *in vivo* grown oocytes that were collected from SAFs and LAFs. HIF1A, SMAD4, and STAT3 are the top upstream regulators that are common for these datasets. These factors are also predicted

Table 1. Comparison between NGS and RT-PCR

Feature ID	NGS Fold difference		RT-PCR Fold difference	
	SAFs/EAFs	LAFs/SAFs	SAFs/EAFs	LAFs/SAFs
GPX7	1.00	–1.11	-	-
FLT1	6.45 *	–2.30 *	6.27 *	–2.67 *
SPP1	7.66 *	–17.63 *	21.85 *	–1.69 *
HIF1A	1.54 *	1.66 *	1.68 *	1.21 *
VEGFA	7.03 *	1.73 *	3.38 *	1.48 *
ACTN4	–2.19 *	–1.15 *	–1.93 *	–1.42 *

* Significant difference ($P < 0.01$). NGS; fold difference of RPKM value between SAFs and EAFs, and between LAFs and SAFs. RT-PCR; relative expression level to GPX7 was compared between SAFs and EAFs, and between LAFs and SAFs.

Table 2. Top five upstream regulators in *in vitro* granulosa cells between SAFs and IVGs and between LAFs and IVGs

No. of best	SAFs - IVGs				LAFs - IVGs			
	Upstream regulator	Activation z-score	P-value of overlap	Predicted activation state	Upstream regulator	Activation z-score	P-value of overlap	Predicted activation state
1	SP1	–1.56	3.26E-26		SP1	–0.47	9.92E-21	
2	TP53	–4.02	4.80E-24	Inhibited	TP53	0.18	1.39E-18	
3	HIF1A	–1.24	2.76E-22		CTNNNB1	–1.68	5.08E-18	
4	SP3	0.46	7.96E-19		HIF1A	–1.46	9.16E-14	
5	FOS	–0.01	1.40E-18		AR	–0.85	2.01E-13	

* The definitions of the terms (Activation z-score, P-value of overlap, and Predicted activation state) are described in the main text.

Table 3. Top five upstream regulators in granulosa cells during *in vivo* follicular development

No. of best	EAFs - SAFs				SAFs - LAFs			
	Upstream regulator	Activation z-score	P-value of overlap	Predicted activation state	Upstream regulator	Activation z-score	P-value of overlap	Predicted activation state
1	SP1	–0.76	4.90E-22		SP1	–2.41	8.72E-22	Inhibited
2	TP53	–2.94	2.49E-17	Inhibited	CTNNB1	–0.44	1.15E-19	
3	HIF1A	0.45	1.17E-14		TP53	–4.05	3.05E-19	Inhibited
4	NR3C1	–1.48	2.83E-14		SP3	–0.27	2.54E-18	
5	STAT3	0.30	5.93E-14		JUN	–1.64	4.03E-17	
others					HIF1A	–2.59	1.99E-09	Inhibited

Table 4. Top five upstream regulators in oocytes between SAFs and IVGs and between LAFs and IVGs

No. of best	SAFs - IVGs				LAFs - IVGs			
	Upstream regulator	Activation z-score	P-value of overlap	Predicted activation state	Upstream regulator	Activation z-score	P-value of overlap	Predicted activation state
1	HIF1A	1.02	2.58E-09		HIF1A	1.94	6.92E-08	
2	SMAD4	1.29	6.57E-08		SMAD4	0.75	1.35E-06	
3	ELK4	-	2.10E-07		TP53	3.59	2.02E-06	activated
4	STAT3	2.54	5.48E-07	activated	STAT3	2.06	2.30E-06	activated
5	VHL	–0.95	2.23E-06		MAFG	–1.91	2.50E-06	

to be key upstream regulators during the development from EAFs to SAFs, whereas only SMAD4 was predicted to be important during the development from SAFs to LAFs (Table 5).

Expression of genes related to OXPHOS, glycolysis, and HIF1A

We found that HIF1 was commonly predicted as a top upstream factor in both granulosa cells and oocytes and as a key regulator of glycolysis and OXPHOS; therefore, we summarized the expression of genes related to glycolysis, OXPHOS, and HIF1 in Table 6. The genes were selected from the Kyoto Encyclopedia of Genes and Genomes pathway database of *Sus scrofa* (http://www.genome.jp/kegg/pathway.html) (Map No. 00010, 00190, and 04066, respectively). In addition, genes with certain expression levels (reads per kilobase of exon per million mapped sequence reads; RPKM > 1.0 during follicle development from EAFs to LAFs) were selected. The number of genes with significantly enhanced or reduced expression was counted for each period of follicle development (EAFs to SAFs, SAFs to LAFs, and SAFs to IVGs). In our preliminary experiments and previous reports involving the same culture methods [1, 10, 11], oocyte diameter (average 112 μm) and the ability to complete nuclear maturation (42%) were found to be similar to those in oocytes of SAFs. Accordingly, here, we compared gene expression between IVGs and SAFs.

The comparison of the number of differentially expressed genes in granulosa cells between EAFs and SAFs showed that 5.6% (1/18) of glycolysis-associated genes were significantly downregulated, whereas 83.3% (15/18) were upregulated, and the difference between the two values was significant (Chi-square test). This trend continued during the development from SAFs to LAFs (3/18 down versus 13/18 up) and was observed in the comparison between SAFs and IVGs (2/18 down versus 15/18 up). The expression level of *HIF1A* statistically significantly increased 1.5- and 1.7-fold respectively during both follicle development periods: from EAFs to SAFs and from SAFs to LAFs (Supplementary Table 1: online only). Certain HIF1-associated genes (34.1%, 14/41) were significantly

Table 5. Upstream regulators including top five between EAFs and SAFs and between SAFs and LAFs

No. of best	EAFs - SAFs				SAFs - LAFs			
	Upstream regulator	Activation z-score	P-value of overlap	Predicted activation state	Upstream regulator	Activation z-score	P-value of overlap	Predicted activation state
1	TGFB1	–1.36	3.01E-11	Inhibited	ATF5	–1.12	1.29E-05	
2	TP53	–3.12	8.38E-10	Inhibited	WNT3A	–3.02	2.33E-05	
3	ERBB2	–4.84	2.29E-09	Inhibited	2-methoxyestradiol	-	3.17E-05	
4	SP1	–1.61	5.52E-08	Inhibited	retaspimycine	-	7.59E-05	
5	HIF1A	–1.19	6.07E-08	Inhibited	leukotriene D4	-	1.18E-04	
others	SMAD4	–3.22	4.39E-06		HIF1A	-	-	
others	STAT3	1.36	1.36E-02	Inhibited	SMAD4	–1.80	3.29E-04	
others					STAT3	-	-	

Table 6. Rate of up- or down-regulated genes associated with glycolysis, OXPHOS, and HIF1 in granulosa cells of EAFs, SAFs, LAFs, and IVGs

	Expression pattern	Follicle stages		
		EAFs - SAFs	SAFs - LAFs	SAFs - IVGs
Glycolysis	Down	5.6 (1/18)	16.7 (3/18)	11.1 (2/18)
	Up	83.3 (15/18) *	72.2 (13/18) *	83.3 (15/18) *
OXPHOS	Down	11.4 (8/70)	31.4 (22/70)	54.3 (38/70)
	Up	71.4 (50/70) *	37.1 (26/70)	24.3 (17/70) *
HIF1	Down	34.1 (14/41)	41.5 (17/41)	26.8 (11/41)
	Up	53.7 (22/41)	51.2 (21/41)	53.7 (22/41) *

* Significant difference between number of up- and down-regulated genes. $P < 0.05$; (Chi-squared test).

Table 7. Rate of up- or down-regulated genes associated with glycolysis, OXPHOS, and HIF1 in oocytes of EAFs, SAFs, LAFs, and IVGs

	Expression pattern	Follicle stages		
		EAFs - SAFs	SAFs - LAFs	SAFs - IVGs
Glycolysis	Down	46.7 (7/15)	26.7 (4/15)	20.0 (3/15)
	Up	26.7 (4/15)	20.0 (3/15)	33.3 (5/15)
OXPHOS	Down	45.1 (32/71)	21.1 (15/71)	21.1 (15/71)
	Up	25.4 (18/71) *	38.0 (27/71) *	33.8 (24/71)
HIF1	Down	64.7 (22/34)	38.2 (13/34)	32.4 (11/34)
	Up	5.9 (2/34) *	2.9 (1/34) *	2.9 (1/34) *

* Significant difference between number of up- and down-regulated genes. $P < 0.05$; (Chi-squared test).

downregulated, whereas 53.7% (22/41) were upregulated during the development from EAFs to SAFs; however, the difference was not statistically significant ($P = 0.075$, Table 6). In addition, expression of the genes associated with HIF1 was enhanced more strongly in IVGs than in SAFs (Table 6). The present analysis shows that 11.4% (8/70) of OXPHOS-associated genes were significantly downregulated, whereas 71.4% (50/70) were upregulated (Table 6). This trend diminished during the development from SAFs to LAFs (Table 6). In contrast to the *in vivo* development, expression levels of OXPHOS-associated genes were greater for IVGs than for SAFs.

In the case of oocytes, no obvious differences in expression of glycolysis-associated genes were observed between *in vivo* and *in vitro* grown oocytes (Table 7), whereas genes associated with HIF1 were significantly downregulated (EAFs–SAFs: down 64.7%, up 5.9%; SAFs–LAFs: down 38.2% and up 2.9%). In addition, the expression of the genes was low in IVGs as compared with oocytes in SAFs (down 32.4% and up 2.9%). Expression levels of OXPHOS-associated genes decreased during development from EAFs to SAFs (32/71 down, 18/71 up, $P < 0.05$) and increased during development from SAFs to LAFs (15/71 down, 27/71 up; Table 7).

Comparison of upstream regulators in granulosa cells and oocytes between follicle development from EAFs to SAFs and from EAFs to IVGs

Table 8 shows the comparison of upstream regulators between *in vivo* and *in vitro* development of oocytes and granulosa cells of OGCs. According to comparison of granulosa cells between EAFs and SAFs (*in vivo* development), 16 regulators were significantly inhibited, nine of which were also identified as "inhibited" in the comparison between EAFs and IVGs (*in vitro* development). In addition, 12 regulators were predicted to be activated during *in vivo* development, and only three (ARNT, HDAC4, and TBX2) were identified as "activated" during *in vitro* development. In contrast, IRF5, IRF7, ETS2, and STAT2 were identified as "inhibited" between EAFs and IVGs (*in vitro* development, Table 8). To find out why for the factors were adversely affected in IVGs, expression of the genes associated with IRF5, IRF7, ETS2, and STAT2 (IRF5: *CXCL10*, *IFIT1*, *IFIT2*, *IFIT3*, *IRF5*, *IRF7*, *ISG15*, *OAS1*, *OAS2*, *PMAIP1*, and *TNFSF10*; IRF7: *ATF4*, *CXCL10*, *DNAJA1*, *IFI35*, *IFIT1*, *IFIT2*, *IFIT3*, *IRF1*, *IRF7*, *IRF8*, *ISG15*, *MCL1*, *MX2*, *OAS1*, *OAS2*, *PARP14*, *PMAIP1*, *TNFSF10*, and *ZBP1*; ETS2: *CD34*, *CSF1R*, *FLT1*, *HPSE*, *MMP13*, *MMP3*, *MMP9*, *MSR1*, *MYC*, *PCSK6*, *PLAU*, and *PTHLH*, *SPP1*; STAT2: *BCL2*, *IFI35*, *IFIT1*, *IFIT2*, *IFIT3*, *IRF1*, *IRF5*, *IRF7*, *ISG15*, *OAS1*, *OAS2*, and *TNFSF10*) was examined (Supplementary Table 1). We found that *FLT1*, *SPP1*, *CD34*, *IFI35*, *OAS2, IFIT1*, *PCSK6*,

Table 8. Comparison of up- and down-regulated upstream regulators between EAFs and SAFs and between EAFs and IVGs

Upstream regulator	EAFs - SAFs		EAFs -IVGs	
	Predicted activation state	Activation z-score	Predicted activation state	Activation z-score
IRF5	Activated	2.74	Inhibited	–3.58
SPI1	Activated	2.61		0.52
ARNT	Activated	2.60	Activated	2.67
HDAC4	Activated	2.41	Activated	2.62
FHL2	Activated	2.40		0.75
TCF7L2	Activated	2.20		1.72
ETS2	Activated	2.16	Inhibited	–2.36
RUNX2	Activated	2.12		0.93
TBX2	Activated	2.11	Activated	2.50
IRF7	Activated	2.06	Inhibited	–5.14
HDAC1	Activated	2.05		0.97
STAT2	Activated	2.04	Inhibited	–2.43
POU3F2	Inhibited	–2.00		-
STAT4	Inhibited	–2.07	Inhibited	–2.78
NEUROG1	Inhibited	–2.13		-
BMI1	Inhibited	–2.18		–1.96
NEUROG3	Inhibited	–2.18		-
NEUROD1	Inhibited	–2.19		-
NUPR1	Inhibited	–2.28	Inhibited	–4.57
ATF6	Inhibited	–2.39		–1.44
RXRB	Inhibited	–2.41		-
XBP1	Inhibited	–2.49	Inhibited	–2.13
CREB1	Inhibited	–2.56	Inhibited	–3.19
ATF4	Inhibited	–2.64	Inhibited	–2.79
SMARCB1	Inhibited	–2.69	Inhibited	–4.53
TP53	Inhibited	–2.94	Inhibited	–5.45
NFE2L2	Inhibited	–3.26	Inhibited	–2.57
CREM	Inhibited	–3.34	Inhibited	–2.38

and *ISG15* had a high expression level (RPKM > 1.0) at the EAF stage, which increased during development from EAFs to SAFs but significantly decreased during development from EAFs to IVGs.

During follicular development from EAFs to SAFs, 54 upstream activators were detected in oocytes. Only two of them were found to be activated during the *in vitro* oocyte development, whereas none was identified as inhibited. In addition, 165 upstream suppressors were predicted during the *in vivo* oocyte development from EAFs to SAFs, 12 of which were identified as inhibited during *in vitro* OGC development, whereas none was identified as activated.

Discussion

The present analysis revealed several possible crucial regulators in granulosa cells and oocytes during *in vivo* follicle development and showed several casual factors of the poorer development of OGCs *in vitro* than *in vivo*.

The present comparison of gene expression patterns in granulosa cells and oocytes between *in vivo* and *in vitro* developing OGCs showed that TP53, SP1, and HIF1 and STAT3, SMAD4, and HIF1 are commonly predicted as top upstream regulators, respectively. The gene expression in bovine granulosa cells collected from three different phases of follicle development was examined previously, and *TP53* and *SP1* were shown to be the main upstream factors between the growth and plateau phases [12]. In the comparison of oocytes with expanded cumulus cells and those with compact cumulus cells, expression of *STAT3* was detected in oocytes associated with high developmental competence [13]. Although it was reported that the deletion of *SMAD4* using *Gdf9-icre* results in a slight but significant reduction in litter size in mice [14], the weaker contribution of this factor to bovine oocyte development was also reported [15]. Here, the expression level of *SMAD4* was high during follicular development and gradually but significantly increased from EAFs to LAFs (RPKM values of EAFs, SAFs, and LAFs, are 6720, 6885, and 7473, respectively). The molecular significance of SMAD4 in follicle development still needs to be elucidated.

HIF1 is a basic helix-loop-helix transcription factor consisting of a heterodimeric complex of α (HIF1A) and β (ARNT) subunits. HIF1A is stable under hypoxic conditions but becomes unstable and is targeted by the ubiquitin-proteasome pathway in the pres-

ence of oxygen. HIF1 plays diverse roles in cellular adaptation for atmospheric conditions and changes the cellular metabolism mechanism from OXPHOS to glycolysis [9]. In addition, cellular adaptation to the culture milieu including atmospheric and energy substrates is a key factor for viability and development of cells. The present analysis showed that glycolysis-associated genes were upregulated in the granulosa cells during follicle development from EAFs to LAFs, suggesting that upregulation of glycolysis is a general trend for granulosa cells during development from EAFs to LAFs. Makanji *et al*. [16] reported that early-stage follicle development is supported by hypoxia-mediated glycolysis, and low-oxygen cultivation of follicles enhances the expression of genes associated with glycolytic enzymes (*Pgk1*, *Hmox1*, *Hk2*, *Gpi*, *Pfkl*, *Pfkp*, *Aldoa*, *Gapdh*, *Pgam1*, *Eno1*, *Pkm*, and *Ldha*). In the present comparison, of the 12 genes, we could not detect *Aldoa*, and the remaining 11 genes were significantly upregulated during development from EAFs to SAFs (Supplementary Table 1). In addition, HIF1 is known to activate the expression of *GLUT 1* (*SLC2A1*) and *GLUT3* (*SLC2A3*) in cancer cells [9]. Our results show that the expression level of *SLC2A3* is very high in granulosa cells of SAFs (RPKM: 671.9), whereas expression levels of *SLC2A1*, *GLUT 4_1* (*SLC2A4_1*), and *GLUT 4_2* (*SLC2A4_2*) were low (RPKM: undetectable, 0.33, and 1.11, respectively; Supplementary Table 1). The expression levels significantly increased during development from EAFs to SAFs for *GLUT 3*, suggesting that high glucose uptake corresponds to high glycolytic activity. Hypoxia activates glycolysis [17], and the present gene analysis revealed that HIF1-associated genes tend to be upregulated during follicle development ($P = 0.075$). The granulosa cell number reportedly determines the concentration of oxygen in follicles [4]. Thus, we believe that during granulosa cell proliferation, dense follicular cells in SAFs may induce hypoxic conditions, which stabilize HIF1 expression and regulate downstream signaling, including that related to glycolysis. For example, VEGFA is a major downstream effector of HIF1A and participates in folliculogenesis [18, 19]. Our analysis showed that the expression levels of *VEGFA* increased 7.0- and 1.7-fold during the two follicle transition periods: from EAFs to SAFs and from SAFs to LAFs, respectively (Supplementary Table 1). Furthermore, Rico *et al*. reported that HIF1 activation is detectable for FSH-regulated *VEGFA* in mice [20]. Thus, FSH is also considered a causal factor of high glycolytic and hypoxic metabolism of granulosa cells. The present study showed that expression of genes associated with HIF1 was enhanced more strongly in IVGs than in SAFs (Table 6). Keeping in mind that there were no differences in the expression of HIF1-associated genes between SAFs and LAFs, we can hypothesize that granulosa cells cultured *in vitro* are more hypoxic than OGCs grown *in vivo*. Similarly, the expression of genes associated with glycolysis was significantly enhanced in IVGs as compared with SAFs (Table 6), and expression levels of *VEGFA* were significantly higher for IVGs than for SAFs (2.3-fold, $P < 0.05$). Therefore, enlargement of follicle size during angiogenesis in follicle development, well-orchestrated management of the granulosa cell number, oxygen provision, and the volume of the culture medium are crucial for OGC development if we consider the of granulosa cell proliferation.

The metabolic switch from OXPHOS to glycolysis is regulated by HIF1A [21], but the present analysis showed significant upregulation of OXPHOS-associated genes in granulosa cells during *in vivo* follicle development from EAFs to SAFs, and this trend diminished during the period SAFs–LAFs. The activation of both OXPHOS and glycolysis was unexpected, and the possible reason for this discrepancy is unclear. Nevertheless, the inner-follicle state of granulosa cells depends on the location [22], and some reports suggest that even cancer cells, which are believed to prefer glycolysis [23], show active oxidative phosphorylation [24]. In the present analysis, we could not determine the inner follicular location of OGCs. Thus, differential characteristics of granulosa cells are mixed, or active phosphorylation is also important for granulosa cells for production of ATP: these questions should be addressed in future studies. When the gene expression pattern of granulosa cells of IVGs was compared to that of SAFs, the genes associated with OXPHOS were found to significantly inactive (Table 6). Therefore, we believe that *in vitro* culture conditions lacking oxygen and energy substrate provision may hamper activation of OXPHOS.

In the case of oocytes, genes associated with HIF1 were significantly downregulated, and the expression of the genes was weak in IVGs in comparison with oocytes in SAFs (down 32.4% and up 2.9%). Therefore, inactivation of HIF1-associated genes seems to be a common feature of oocytes during follicle development. The activity of OXPHOS-related genes significantly decreased during follicle development from EAFs to SAFs but increased during development from SAFs to LAFs, pointing to changes in oocyte energy metabolism during follicle development.

Here, we compared upstream regulators between *in vivo* and *in vitro* development of oocytes and of granulosa cells of OGCs, and found that *FLT1*, *SPP1*, *CD34*, *IFI35*, *OAS2 IFIT1*, *PCSK6*, and *ISG15* have different expression patterns between the periods EAFs–SAFs and EAFs–IVGs. Thus, these factors can be considered key determinants of differences in the features of granulosa cells between *in vivo* and *in vitro* conditions. FLT1 (which belongs to the VEGF receptor family) reportedly improves follicle development [25, 26]. Given our finding that *VEGFA* expression increased during both periods (EAFs–SAFs and EAFs–IVGs: 7.0- and 2.3-fold, respectively), a decrease in the receptor level is a causal factor of impaired *in vitro* development of OGCs. Expression of *SPP1* (osteopontin) increases during follicle development [27]. *SPP1* increases interferon γ expression [28], and it is noteworthy that the above-mentioned genes that were adversely affected under *in vitro* conditions are interferon-associated genes. These genes were significantly downregulated during follicular development from EAFs to IVGs but upregulated in the period EAFs–SAFs. Lédée *et al*. [29] reported that interferon γ in follicular fluid is highly expressed for human embryos that cleaved early. These results as well as the previous report indicate that low expression levels of the genes related to interferons may be the major determinants of the poor *in vitro* development of OGCs. PCSK6, a member of the proprotein convertase family, is involved in inhibition of apoptosis of granulosa cells in preovulatory human follicles [30], and *PCSK6*-mutant mice show a loss of ovarian function [31]; these data are suggestive of low expression of the genes associated with impaired development of OGCs.

During follicular development from EAFs to SAFs, we identified a large number of upstream regulators in *in vivo* developing oocytes

but observed a similar trend in a small fraction of the upstream factors during period EAFs–IVGs. The extent of differences between *in vivo* and *in vitro* conditions indicates that the conditions of oocytes grown *in vitro* differ strongly from those of *in vivo* grown oocytes.

In conclusion, follicle development from EAFs to AFs requires granulosa proliferation, which is likely supported by activation of the glycolysis pathway; cultivation of OGCs *in vitro* changes the pattern of gene expression (in comparison with those in *in vivo* developing OGCs).

Acknowledgments

This study was supported by the Promotion and Mutual Aid Corporation for Private Schools of Japan and the Ministry of Education, Culture, Sports, Science, and Technology (Grant-in-Aid for Scientific Research # S0801025) and by the Grant-in-Aid for Scientific Research C (KAKENHI, grant No. 25450400) from the Japan Society for the Promotion of Science.

References

1. **Oi A, Tasaki H, Munakata Y, Shirasuna K, Kuwayama T, Iwata H.** Effects of reaggregated granulosa cells and oocytes derived from early antral follicles on the properties of oocytes grown *in vitro*. *J Reprod Dev* 2015; **61**: 191–197. [Medline] [CrossRef]
2. **Orisaka M, Tajima K, Tsang BK, Kotsuji F.** Oocyte-granulosa-theca cell interactions during preantral follicular development. *J Ovarian Res* 2009; **2**: 9. [Medline] [CrossRef]
3. **van Wezel IL, Rodgers RJ.** Morphological characterization of bovine primordial follicles and their environment *in vivo*. *Biol Reprod* 1996; **55**: 1003–1011. [Medline] [CrossRef]
4. **Li D, Redding GP, Bronlund JE.** Oxygen consumption by bovine granulosa cells with prediction of oxygen transport in preantral follicles. *Reprod Fertil Dev* 2013; **25**: 1158–1164. [Medline] [CrossRef]
5. **Redding GP, Bronlund JE, Hart AL.** Mathematical modelling of oxygen transport-limited follicle growth. *Reproduction* 2007; **133**: 1095–1106. [Medline] [CrossRef]
6. **Redding GP, Bronlund JE, Hart AL.** Theoretical investigation into the dissolved oxygen levels in follicular fluid of the developing human follicle using mathematical modelling. *Reprod Fertil Dev* 2008; **20**: 408–417. [Medline] [CrossRef]
7. **Van Blerkom J, Antczak M, Schrader R.** The developmental potential of the human oocyte is related to the dissolved oxygen content of follicular fluid: association with vascular endothelial growth factor levels and perifollicular blood flow characteristics. *Hum Reprod* 1997; **12**: 1047–1055. [Medline] [CrossRef]
8. **Kroemer G, Pouyssegur J.** Tumor cell metabolism: cancer's Achilles' heel. *Cancer Cell* 2008; **13**: 472–482. [Medline] [CrossRef]
9. **Courtnay R, Ngo DC, Malik N, Ververis K, Tortorella SM, Karagiannis TC.** Cancer metabolism and the Warburg effect: the role of HIF-1 and PI3K. *Mol Biol Rep* 2015; **42**: 841–851. [Medline] [CrossRef]
10. **Tasaki H, Iwata H, Sato D, Monji Y, Kuwayama T.** Estradiol has a major role in antrum formation of porcine preantral follicles cultured *in vitro*. *Theriogenology* 2013; **79**: 809–814. [Medline] [CrossRef]
11. **Itami N, Shirasuna K, Kuwayama T, Iwata H.** Resveratrol improves the quality of pig oocytes derived from early antral follicles through sirtuin 1 activation. *Theriogenology* 2015; **83**: 1360–1367. [Medline] [CrossRef]
12. **Douville G, Sirard MA.** Changes in granulosa cells gene expression associated with growth, plateau and atretic phases in medium bovine follicles. *J Ovarian Res* 2014; **7**: 50. [Medline] [CrossRef]
13. **Mohammadi-Sangcheshmeh A, Held E, Rings F, Ghanem N, Salilew-Wondim D, Tesfaye D, Sieme H, Schellander K, Hoelker M.** Developmental competence of equine oocytes: impacts of zona pellucida birefringence and maternally derived transcript expression. *Reprod Fertil Dev* 2014; **26**: 441–452. [Medline] [CrossRef]
14. **Li X, Tripurani SK, James R, Pangas SA.** Minimal fertility defects in mice deficient in oocyte-expressed Smad4. *Biol Reprod* 2012; **86**: 1–6. [Medline] [CrossRef]
15. **Kaune H, Peyrache E, Williams SA.** Oocyte-derived Smad4 is not required for development of the oocyte or the preimplantation embryo. *Theriogenology* 2015; **83**: 897–903. [Medline] [CrossRef]
16. **Makanji Y, Tagler D, Pahnke J, Shea LD, Woodruff TK.** Hypoxia-mediated carbohydrate metabolism and transport promote early-stage murine follicle growth and survival. *Am J Physiol Endocrinol Metab* 2014; **306**: E893–E903. [Medline] [CrossRef]
17. **Yee Koh M, Spivak-Kroizman TR, Powis G.** HIF-1 regulation: not so easy come, easy go. *Trends Biochem Sci* 2008; **33**: 526–534. [Medline] [CrossRef]
18. **Grasselli F, Basini G, Bussolati S, Tamanini C.** Effects of VEGF and bFGF on proliferation and production of steroids and nitric oxide in porcine granulosa cells. *Reprod Domest Anim* 2002; **37**: 362–368. [Medline] [CrossRef]
19. **Doyle LK, Walker CA, Donadeu FX.** VEGF modulates the effects of gonadotropins in granulosa cells. *Domest Anim Endocrinol* 2010; **38**: 127–137. [Medline] [CrossRef]
20. **Rico C, Dodelet-Devillers A, Paquet M, Tsoi M, Lapointe E, Carmeliet P, Boerboom D.** HIF1 activity in granulosa cells is required for FSH-regulated Vegfa expression and follicle survival in mice. *Biol Reprod* 2014; **90**: 135. [Medline] [CrossRef]
21. **Chen CT, Hsu SH, Wei YH.** Mitochondrial bioenergetic function and metabolic plasticity in stem cell differentiation and cellular reprogramming. *Biochim Biophys Acta* 2012; **1820**: 571–576. [Medline] [CrossRef]
22. **Russo V, Berardinelli P, Martelli A, Di Giacinto O, Nardinocchi D, Fantasia D, Barboni B.** Expression of telomerase reverse transcriptase subunit (TERT) and telomere sizing in pig ovarian follicles. *J Histochem Cytochem* 2006; **54**: 443–455. [Medline] [CrossRef]
23. **Cantor JR, Sabatini DM.** Cancer cell metabolism: one hallmark, many faces. *Cancer Discov* 2012; **2**: 881–898. [Medline] [CrossRef]
24. **Rodríguez-Enríquez S, Hernández-Esquivel L, Marín-Hernández A, El Hafidi M, Gallardo-Pérez JC, Hernández-Reséndiz I, Rodríguez-Zavala JS, Pacheco-Velázquez SC, Moreno-Sánchez R.** Mitochondrial free fatty acid β-oxidation supports oxidative phosphorylation and proliferation in cancer cells. *Int J Biochem Cell Biol* 2015; **65**: 209–221. [Medline] [CrossRef]
25. **Shimizu T, Jiang JY, Iijima K, Miyabayashi K, Ogawa Y, Sasada H, Sato E.** Induction of follicular development by direct single injection of vascular endothelial growth factor gene fragments into the ovary of miniature gilts. *Biol Reprod* 2003; **69**: 1388–1393. [Medline] [CrossRef]
26. **Celik-Ozenci C, Akkoyunlu G, Kayisli UA, Arici A, Demir R.** Localization of vascular endothelial growth factor in the zona pellucida of developing ovarian follicles in the rat: a possible role in destiny of follicles. *Histochem Cell Biol* 2003; **120**: 383–390. [Medline] [CrossRef]
27. **Skinner MK, Schmidt M, Savenkova MI, Sadler-Riggleman I, Nilsson EE.** Regulation of granulosa and theca cell transcriptomes during ovarian antral follicle development. *Mol Reprod Dev* 2008; **75**: 1457–1472. [Medline] [CrossRef]
28. **Shan M, Yuan X, Song LZ, Roberts L, Zarinkamar N, Seryshev A, Zhang Y, Hilsenbeck S, Chang SH, Dong C, Corry DB, Kheradmand F.** Cigarette smoke induction of osteopontin (SPP1) mediates T(H)17 inflammation in human and experimental emphysema. *Sci Transl Med* 2012; **4**: 117ra9. [Medline] [CrossRef]
29. **Lédée N, Lombroso R, Lombardelli L, Selva J, Dubanchet S, Chaouat G, Frankenne F, Foidart JM, Maggi E, Romagnani S, Ville Y, Piccinni MP.** Cytokines and chemokines in follicular fluids and potential of the corresponding embryo: the role of granulocyte colony-stimulating factor. *Hum Reprod* 2008; **23**: 2001–2009. [Medline] [CrossRef]
30. **Wang Y, Wang XH, Fan DX, Zhang Y, Li MQ, Wu HX, Jin LP.** PCSK6 regulated by LH inhibits the apoptosis of human granulosa cells via activin A and TGFβ2. *J Endocrinol* 2014; **222**: 151–160. [Medline] [CrossRef]
31. **Mujoomdar ML, Hogan LM, Parlow AF, Nachtigal MW.** Pcsk6 mutant mice exhibit progressive loss of ovarian function, altered gene expression, and formation of ovarian pathology. *Reproduction* 2011; **141**: 343–355. [Medline] [CrossRef]